

Multiqudit quantum hashing and its implementation based on orbital angular momentum encoding

D O Akat'ev¹, A V Vasiliev^{1,2}, N M Shafeev², F M Ablayev^{1,2},
and A A Kalachev^{1,2}

¹ Zavoisky Physical-Technical Institute, FRC Kazan Scientific Center of RAS, Kazan, Russian Federation

² Kazan Federal University, Kazan, Russian Federation

E-mail: akatevdmirijj@gmail.com, vav.kpfu@gmail.com

October 2022

Abstract. A new version of quantum hashing technique is developed wherein a quantum hash is constructed as a sequence of single-photon high-dimensional states (qudits). A proof-of-principle implementation of the high-dimensional quantum hashing protocol using orbital-angular momentum encoding of single photons is implemented. It is shown that the number of qudits decreases with increase of their dimension for an optimal ratio between collision probability and decoding probability of the hash. Thus, increasing dimension of information carriers makes quantum hashing with single photons more efficient.

Keywords: single-photon states, orbital angular momentum, quantum hashing, SPDC

1. Introduction

Hashing algorithms today have become essential in cybersecurity, cryptography, data-intensive research, etc., as they can reliably inform us whether two files are identical without opening and comparing them. As an important part of cryptography, a hash function compresses a message of any length into a digest of fixed length and it is the key technology of verification of message integrity, digital signatures, fingerprinting and other cryptographic applications [1, 2]. Moreover, a universal hash function is an important part of the privacy amplification process of the quantum key distribution [3]. For such applications, a good hashing algorithm should satisfy two main properties: one-way property and collision resistance. The first means that restoring an input from its hash should be a computationally hard problem. The second property means that the situation when two different inputs have the same hash (such a situation is called a collision) is hard to find.

Recently, a promising generalization of the cryptographic hashing concept on the quantum domain, which is called quantum hashing, has been suggested and developed [4, 5, 6, 7]. In this case, the hash function encodes a classical input state into a quantum

state so that to optimize the trade-off between one-way property and collision resistance. In particular, in [7], it was suggested to construct a quantum hash via a sequence of single-photon qubits, and a proof-of-principle experiment using single photons with orbital angular momentum (OAM) encoding was implemented. In the present paper, we further develop this approach both theoretically and experimentally and construct a quantum hash as a sequence of single-photon high-dimensional states (qudits). We show that the use of high-dimensional states increases the collision resistance of hashing protocols and enhances the resistance against extraction of information about the classical input.

2. Theory

2.1. Preliminaries

In [4] we have proposed a cryptographic quantum hash function and later in [8] provided its generalized version for arbitrary finite abelian groups based on the notion of ε -biased sets. Here we consider its version for a cyclic group \mathbb{Z}_q . In this case, for a set $S \subseteq \mathbb{Z}_q$ we can define its *bias* with respect to $x \in \mathbb{Z}_q$ as following:

$$\text{bias}(S, x) = \frac{1}{|S|} \left| \sum_{s \in S} e^{2\pi s x / q} \right|, \quad (2.1)$$

and the set S is called ε -biased if for any $x \neq 0$ $\text{bias}(S, x) \leq \varepsilon$.

These sets are especially interesting when $|S| \ll |\mathbb{Z}_q|$ (as $S = \mathbb{Z}_q$ is obviously 0-biased). In their seminal paper [9] Naor and Naor defined these small-biased sets, gave the first explicit constructions of such sets, and demonstrated the power of small-biased sets for several applications. Note that ε -biased sets of size $O(\log q / \varepsilon^2)$ exist as proved in [10].

In [4] we have introduced the notion of quantum hashing and its main properties. Later in [6] we have considered the trade-off and balancing between two main properties of quantum hashing, and proposed a more general definition of the quantum (δ, ε) -resistant hash function. Here we recall it in the concise manner and refer for details to [6].

Definition 1 *Let $\delta \in (0, 1]$ and $\varepsilon \in [0, 1)$. We call a function $\psi : \mathbb{X} \rightarrow \mathcal{H}^K$ a quantum (δ, ε) -resistant hash function if it has two main properties:*

(i) δ -one-wayness, i.e.

$$\frac{K}{|\mathbb{X}|} \leq \delta,$$

(ii) ε -collision-resistance, i.e. for any pair x_1, x_2 of different inputs

$$|\langle \psi(x_1) | \psi(x_2) \rangle| \leq \varepsilon.$$

In other words a quantum function ψ encodes an input $x \in \mathbb{X}$ into the quantum state $|\psi(x)\rangle$ of dimension K . The properties of such a function include resistance to inversion

(known as “one-way property” or “preimage resistance”), which makes it unlikely to “extract” encoded information out of the quantum state, and resistance to quantum collisions, which means that quantum images for different inputs can be distinguished with high probability.

Note that the measure of collision resistance (denoted above by ε) is not the probability of quantum collisions. The probability of collisions follows from the particular comparison procedure that we use. It can be the well-known SWAP-test [11], REVERSE-test [12] or simply a result of projection of $|\psi(x_1)\rangle$ onto $|\psi(x_2)\rangle$. In the latter case the probability of collisions would be described by the fidelity between $|\psi(x_1)\rangle$ and $|\psi(x_2)\rangle$, and thus bounded by ε^2 .

2.2. Multiqudit Quantum Hashing

Here we define a new version of the quantum hashing technique for a cyclic group, i.e. we consider $\mathbb{X} = \mathbb{Z}_q$ and $|\mathbb{X}| = q$. It is based on small-biased sets and high-dimensional states (qudits). But first we note the following equivalence between ε -biased sets.

Property 1 *Let $S = \{s_1, \dots, s_d\}$ and $S' = \{0, (s_2 - s_1), \dots, (s_d - s_1)\}$. Then for any $x \in \mathbb{Z}_q$ $\text{bias}(S, x) = \text{bias}(S', x)$, i.e. the set S is equivalent (in terms of its bias) to S' .*

Proof. The proof of this statement is based on the following considerations:

$$\frac{1}{d} \left| \sum_{k=1}^d e^{2\pi s_k x/q} \right| = \frac{1}{d} \left| e^{2\pi s_1 x/q} \sum_{k=1}^d e^{2\pi (s_k - s_1)x/q} \right| = \frac{1}{d} \left| \sum_{k=1}^d e^{2\pi (s_k - s_1)x/q} \right|,$$

therefore

$$\text{bias}(S, x) = \frac{1}{d} \left| \sum_{k=1}^d e^{2\pi s_k x/q} \right| = \frac{1}{d} \left| \sum_{k=1}^d e^{2\pi (s_k - s_1)x/q} \right| = \text{bias}(S', x).$$

□

Now let $S_1, S_2, \dots, S_m \subset \mathbb{Z}_q$ be the ε -biased subsets of \mathbb{Z}_q , and we denote $S_j = \{s_{j,1}, \dots, s_{j,d}\}$ for $j = 1, \dots, m$. By the Property 1 without loss of generality we may consider all $s_{j,1}$ to be equal 0. In other words for all $j = 1, \dots, m$ it holds that

$$\max_{x \neq 0} \frac{1}{d} \left| 1 + e^{i \frac{2\pi s_{j,2} x}{q}} + \dots + e^{i \frac{2\pi s_{j,d} x}{q}} \right| \leq \varepsilon.$$

Then for $x \in \mathbb{Z}_q$ we define a multiqudit quantum hash function in the following way:

$$|\psi_j(x)\rangle = \frac{1}{\sqrt{d}} (|\ell_1\rangle + e^{i2\pi s_{j,2} x/q} |\ell_2\rangle + \dots + e^{i2\pi s_{j,d} x/q} |\ell_d\rangle), \quad (2.2)$$

$$|\psi(x)\rangle = |\psi_1(x)\rangle \otimes \dots \otimes |\psi_m(x)\rangle, \quad (2.3)$$

where $|\ell_k\rangle$ are the basis states ($k = 1 \dots d$, d is the dimension of the qudit state space), q is the size of the input state space, $x \in \{0, 1, \dots, q-1\}$ is a classical input that is encoded by the relative phase of m qudit states, $s_{i,k}$ are numeric parameters (elements of the ε -biased sets) of the quantum hash function that provide its collision resistance. The main

idea of the collision resistance property is to provide minimum fidelity between different quantum hashes (quantum hash function images) with the minimal possible number of quantum information carriers. Furthermore, reaching reasonable balance between collision resistance property and one-way property for a quantum hash function is also an important task.

Note that the formula for $|\psi(x)\rangle$ gives the classical-quantum function that transforms a classical input into the quantum state composed of m qudits (d -dimensional systems). The same state can be constructed with appropriate number of 2-dimensional systems (qubits), however this would imply creating entangled states, which are harder to create and maintain.

Theorem 1 *The classical-quantum function $\psi : \mathbb{Z}_q \rightarrow \mathcal{H}^{d^m}$ given by Eqs. 2.2, and 2.3 is a $\left(\frac{d^m}{q}, \varepsilon^m\right)$ -resistant quantum hash function.*

Proof. According to the definition 1, we need to show two main properties for the function ψ :

- (i) δ -one-wayness. The dimension of the input space is q , the quantum state space has dimension d^m . Thus, ψ is δ -one-way for

$$\delta = \frac{d^m}{q}.$$

- (ii) ε -collision-resistance. The maximal inner product between unequal quantum hashes is bounded by

$$\begin{aligned} \max_{x_1 \neq x_2} |\langle \psi(x_1) | \psi(x_2) \rangle| &= \max_{x_1 \neq x_2} \prod_{j=1}^m \left[\frac{1}{d} \left| 1 + e^{i \frac{2\pi s_{j,2}(x_2-x_1)}{q}} + \dots + e^{i \frac{2\pi s_{j,d}(x_2-x_1)}{q}} \right| \right] \\ &= \max_{x \neq 0} |\langle \psi(x) | \psi(0) \rangle| \\ &= \max_{x \neq 0} \prod_{j=1}^m \left[\frac{1}{d} \left| 1 + e^{i \frac{2\pi s_{j,2}x}{q}} + \dots + e^{i \frac{2\pi s_{j,d}x}{q}} \right| \right] \leq \varepsilon^m, \end{aligned}$$

if all $S_j = \{s_{j,1}, \dots, s_{j,d}\}$ are ε -biased sets.

Thus, ψ corresponds to the balanced $\left(\frac{d^m}{q}, \varepsilon^m\right)$ -resistant quantum hash function according to [6]. \square

Note that the proof above also suggests that comparing hashes of two different values x_1 and x_2 is equivalent to comparing hashes of $x = (x_2 - x_1)$ and 0.

Remark 1 *Although ε -biased sets give guaranteed collision resistance to our multiqudit quantum hash function, for small sizes of input and output spaces better bounds on collision resistance can be obtained by numeric optimization (see Table 1 for details).*

At the moment this approach can be used only for relatively small values of d, m and q since it implies an exhaustive search for optimal values of $s_{j,k}$ that give minimum to the following function:

$$\min_{\{s_{j,k}\}} \max_{x \neq 0} \frac{1}{d^m} \prod_{j=1}^m \left| 1 + e^{i \frac{2\pi s_{j,2}x}{q}} + \dots + e^{i \frac{2\pi s_{j,d}x}{q}} \right|.$$

Table 1. The worst-case values of collision probability with parameters from ε -biased sets and from the numeric optimization, $q = 256$.

Number of qudits	ε -biased sets	Exhaustive search
$d = 2$		
1	0,9998	0,9998
2	0,9996	0,959
3	0,9994	0,7519
4	0,9992	0,4378
5	0,999	0,2031
6	0,9988	0,0806
7	0,9986	0,0279
$d = 3$		
1	0,9681	0,9681
2	0,9372	0,5422
3	0,9073	0,1483
4	0,8784	0,0368
5	0,8504	0,0063
$d = 4$		
1	0,8329	0,8329
2	0,6937	0,2174
3	0,5778	0,0429
4	0,4813	0,0072

3. Experiment

3.1. Single-photon states with an orbital angular momentum

As we have shown above, the construction of the multiqudit quantum hash function (2.3) is adapted for implementation by the sequence of high-dimensional states (qudits) with specific encoding. For that purposes we use single photons with an orbital angular momentum (OAM) generated via spontaneous parametric down-conversion (SPDC). OAM-based encoding is currently widely used for implementing various quantum communication protocols (see, e.g., the reviews [13, 14]) and is especially promising for their high-dimensional variants [15].

In the process of SPDC [16, 17], when a pump beam propagates through a quadratic nonlinear medium, one of the pump photons spontaneously annihilates and signal and idler photons are simultaneously created. The signal and idler photons have to satisfy the phase matching conditions $\omega_p = \omega_s + \omega_i$ and $\vec{k}_p = \vec{k}_s + \vec{k}_i + \vec{k}_{QPM}$, where ω_j and \vec{k}_j are the frequency and wave vector, respectively, corresponding to the pump ($j = p$),

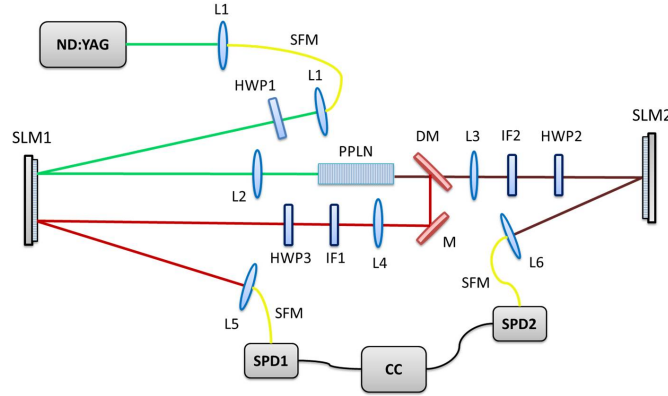


Figure 1. The experimental setup for single-photon qudit generation.

signal ($j = s$) and idler ($j = i$) photons, and \vec{k}_{QPM} is a so called quasiphasematching vector ($k_{QPM} = 2\pi/\Lambda$) for a crystal poling with period Λ . If the pump radiation has an orbital angular momentum l_p and all the photons propagate in the same direction (collinear SPDC), then the generated photon pairs also have OAM [18, 19] satisfying to the conservation law

$$l_p = l_s + l_i. \quad (3.1)$$

In the present work, we created single-photon qudit states by projecting the angular momentum of the idler photons onto the mode with $l_i = 0$. In this case, since $l_p = l_s$, the spatial structure of the signal photon reproduces that of the pump field. To construct the multiqudit version of the quantum hash function we exploit single-photon qudits in a superposition of Laguerre-Gaussian (LG_p^l) modes with the radial index $p = 0$. In particular, we focus on the equally weighted superpositions that have the following form:

$$|\psi\rangle = \frac{1}{\sqrt{d}}(|\ell_1\rangle + e^{i\varphi_2}|\ell_2\rangle + \dots + e^{i\varphi_d}|\ell_d\rangle), \quad (3.2)$$

where $|\ell_n\rangle$ denotes a single-photon state corresponding to $LG_0^{\ell_n}$ mode, $n = 1 \dots d$, where d is the dimension of the qudit state space, and φ_n is a relative phase.

Our experimental setup is schematically shown in figure 1. We use a 2 cm long type-0 periodically poled $\text{LiNbO}_3:\text{MgO}$ 5% (PPLN) crystal with a period of $7.50 \mu\text{m}$, which is designed to generate signal photons at wavelength of 810 nm and idler photons at 1550 nm from a pump field at wavelength of 532 nm (CW ND-YAG) under 75°C operation temperature. The pump field is spatially filtered by a single-mode fiber (SMF) interfaced by two lenses (L1). To prepare required spatial states of the pump field we take advantage of a phase holography technique developed in [20], where the required modes are obtained after beam reflection from SLM's screen and picked out the first diffraction order. The first SLM1 (Holoeye PLUTO-2) convert the Gaussian pump beam into an LG mode (part 1 of SLM1) and detect signal photons (part 2 of SLM1) using the phase-flattening technique [18]. The half-wave plates (HWP_i , where $i = 1, 2, 3$) was used to optimize the field polarization with respect to the SLMs. After the preparation of the

required LG mode, the pump beam is sent through the PPLN crystal using the biconvex lens L2 with the focal length of 17.5 cm. The signal and idler photons, generated at the wavelength of 810 nm and 1550 nm, respectively, are separated by a dichroic mirror (DM). In the idler arm, the photons are collimated using a lens L3 with the focal length of 150 mm. After that, the idler photons are sent to SLM2, which maintains only $\ell = 0$ mode, and are coupled by the aspheric lens L6 with the focal length of 11 mm into a single mode fiber SMF. As a result, the detected photons have only zero OAM ($\ell_i = 0$). In the signal arm, the photons are collimated using the lens L4 with the focal length of 150 mm and are sent to the part 2 of SLM1. Having been transformed they are coupled by the aspheric lens L5 with the focal length of 11 mm into a SMF. Interference filters IF1 and IF2 are used to select photons at signal and idler wavelengths, respectively.

The focal length of L2 was chosen to approach the single-Schmidt mode regime of SPDC [21]. In the single-Schmidt mode regime, the Rayleigh range of the pump beam $z_r = (\pi w^2)/\lambda$ should be equal to half of the crystal length L . Following this criteria, we estimated the required pump beam waist to be $w_p = 29 \mu\text{m}$. For the optimal detection of the down-converted modes, the lenses L3 and L4 were chosen so that the Rayleigh range of the signal and idler beams be equal to half of the crystal length L , which requires $w_s = 36 \mu\text{m}$ and $w_i = 50 \mu\text{m}$. In the experiment we had $w_p = 32 \pm 0.7 \mu\text{m}$, $w_s = 40.3 \pm 1.2 \mu\text{m}$, and $w_i = 50.1 \pm 0.51 \mu\text{m}$.

The photon detection was carried out using photodetectors SPD1 (SPCM AQR-14, PerkinElmer) operating in the free running mode with an efficiency of 45%, dark count rate of the order of 2 kHz and dead time of 150 ns, and SPD2 (ID Quantique 210) operating in the free running mode with an efficiency of 10%, dark count rate of the order of 15 kHz, and dead time of 16 μs . The signals from both detectors are analyzed by the time-to-digital converter (CC, Time Tagger 20).

To explore quantum hashing main properties we prepared quantum states with the dimension $d = 2, 3$, and 4 in the basis of OAM modes $\ell = -3, -2, \dots, 3$. The examples of these states are

$$|\psi_j^{d=2}(\phi_1)\rangle = \frac{1}{\sqrt{2}} (|2\rangle + e^{i\phi_1}|-2\rangle), \quad (3.3)$$

$$|\psi_j^{d=3}(\phi_2, \phi_3)\rangle = \frac{1}{\sqrt{3}} (|2\rangle + e^{i\phi_2}|-2\rangle + e^{i\phi_3}|0\rangle), \quad (3.4)$$

$$|\psi_j^{d=4}(\phi_4, \phi_5, \phi_6)\rangle = \frac{1}{\sqrt{4}} (|3\rangle + e^{i\phi_4}|-3\rangle + e^{i\phi_5}|1\rangle + e^{i\phi_6}|-1\rangle). \quad (3.5)$$

To determine states quality we take advantage of the quantum tomography approach developed in [22, 23]. As an example, we present here quantum tomographic measurements for the qutrit state $|\psi_j^{d=3}(0, 0)\rangle$, which illustrate the accuracy of our experiment. The reconstructed density matrix $\rho_{|\psi_j^{d=3}(0,0)\rangle}^{exp} = \rho_{real}^{exp} + \rho_{imag}^{exp}$ is

$$\rho_{real}^{exp} = \begin{pmatrix} 0.332 \pm 0.002 & 0.328 \pm 0.005 & 0.33 \pm 0.005 \\ 0.328 \pm 0.005 & 0.344 \pm 0.01 & 0.332 \pm 0.002 \\ 0.33 \pm 0.005 & 0.332 \pm 0.002 & 0.344 \pm 0.009 \end{pmatrix}, \quad (3.6)$$

$$\rho_{imag}^{exp} \begin{pmatrix} 0 & (0.002 \pm 0.003)i & (0.002 \pm 0.003)i \\ (-0.002 \mp 0.003)i & 0 & -(0.002 \pm 0.001)i \\ (-0.002 \mp 0.003)i & (0.002 \pm 0.001)i & 0 \end{pmatrix}. \quad (3.7)$$

The main figure of merit is the fidelity, which is a measure of how close the reconstructed state is to a target state and is given by $F = [Tr(\sqrt{\sqrt{\rho_{target}}\rho^{exp}\sqrt{\rho_{target}}})]^2$, where ρ_{target} and ρ^{exp} are the target and reconstructed density matrices, respectively [24]. We have found that $F_{d=3} = 0.987 \pm 0.012$. In the same way, we estimated that fidelity for the qubit state $|\psi_j^{d=2}(\frac{2\pi}{3})\rangle$ is $F_{d=2} = 0.99 \pm 0.01$. To determine the purity of these state we calculated the eigenvalues of the density matrices. The largest eigenvalues were $\lambda_{d=2} = 0.999$ and $\lambda_{d=3} = 0.993$ that correspond to high purity states. As a result, based on the experimental data we can conclude that quantum states of different dimensions are prepared with high purity and high accuracy level.

3.2. Implementation of the multiqudit quantum hashing

In the previous work [7], we have suggested quantum hash functions as a sequence of independent qubits, where classical information was encoded into qubits phase. Now we propose quantum hashing protocol, where the information carriers are high-dimensional states with an orbital angular momentum. In this case, the structure of the quantum hash can be represented by Eqs. 2.2, and 2.3.

Here we propose the implementation of the verification procedure that for a given quantum hash $|\psi(x_1)\rangle$ and a classical value x_2 checks whether $x_1 = x_2$ or not. The ideal quantum experiment that verifies a multiqudit quantum hash can be set as follows.

- (i) We receive a quantum hash of some generally unknown value x_1 as a sequence of m single photons in the overall state $|\psi(x_1)\rangle$:

$$|\psi(x_1)\rangle = |\psi_1(x_1)\rangle \otimes \dots \otimes |\psi_m(x_1)\rangle,$$

where the j -th qudit is expected to be in the state $|\psi_j(x_1)\rangle$ as described by equation (2.2).

- (ii) Then we check whether x_1 equals to some predefined x_2 or not. To do this we perform measurements that project $|\psi_j(x_1)\rangle$ onto $|\psi_j(x_2)\rangle$ and $d - 1$ phase orthogonal states

$$|\psi_j^{\perp,g}(x_2)\rangle = \frac{1}{\sqrt{d}}(|\ell_1\rangle + e^{i\frac{2\pi s_{j,2}x_2}{q} + i\phi_{g,2}}|\ell_2\rangle + \dots + e^{i\frac{2\pi s_{j,d}x_2}{q} + i\phi_{g,d}}|\ell_d\rangle), \quad (3.8)$$

where $|\langle\psi_j(x_2)|\psi_j^{\perp,g}(x_2)\rangle|^2 = 0$, $g = 1, \dots, d - 1$, and $\phi_{g,d}$ are additional phases responsible for orthogonality of the states. For example, if we use the qutrits (3-dimensional states) as information carriers, the set of $\{\phi_{g,d}\}$ is equal to $\{\{2\pi/3, -2\pi/3\}, \{-2\pi/3, 2\pi/3\}\}$.

- (iii) The projection measurements of these states may be sequential or parallel. In the latter case we have to prepare a complex phase mask on the part 2 of SLM1 which is an appropriate superposition of detection masks for $|\psi_j(x_2)\rangle$ and $d - 1$

states $|\psi_j^{\perp,g}(x_2)\rangle$. The complex mask directs the photons into d detection channels corresponding to the states $|\psi_j(x_2)\rangle, |\psi_j^{\perp,1}(x_2)\rangle, \dots, |\psi_j^{\perp,d-1}(x_2)\rangle$, respectively. The single-photon detector click in $|\psi_j(x_2)\rangle$ or $|\psi_j^{\perp,g}(x_2)\rangle$ channels corresponds to the outcome $|\psi_j(x_1)\rangle = |\psi_j(x_2)\rangle$ or $|\psi_j(x_1)\rangle \neq |\psi_j(x_2)\rangle$, respectively.

- (iv) If $x_1 = x_2$, the detector of the output $|\psi_j(x_2)\rangle$ would always click, while the other detectors would never click.
- (v) If $x_1 \neq x_2$, each of the detectors might click, but the probability of erroneous outcome “ $x_1 = x_2$ ” is bounded by the construction of the quantum hash function $|\psi(x)\rangle$.
- (vi) If none of the detectors had clicked, then the qudit is lost, and we either request its resending or tolerate the higher error probability.
- (vii) If all of m measurements end up with the outcome “ $|\psi_j(x_1)\rangle = |\psi_j(x_2)\rangle$ ”, then the final result of the experiment is considered to be “ $x_1 = x_2$ ”. Otherwise, if at least one qudit leads to $|\psi_j(x_1)\rangle \neq |\psi_j(x_2)\rangle$, then the overall result is also “ $x_1 \neq x_2$ ”.

The error probability comes from the fidelity between two different quantum hashes, which is

$$|\langle\psi(x_1)|\psi(x_2)\rangle|^2 = \frac{1}{d^{2m}} \prod_{j=1}^m \left| 1 + e^{i\frac{2\pi s_{j,2}(x_1-x_2)}{q}} + \dots + e^{i\frac{2\pi s_{j,d}(x_1-x_2)}{q}} \right|^2. \quad (3.9)$$

The parameter set $\{s_{j,k}\}$ is chosen in such a way that the pairs of hashes $|\psi(x_1)\rangle$ and $|\psi(x_2)\rangle$ give the minimal fidelity for $x_1 \neq x_2$. To measure the collision probability we compare different quantum hashes in the worst-case scenario when quantum hashes for x_1 and x_2 have the maximum fidelity for a given set $\{s_{j,k}\}$.

The protocol starts with a calibration step on which we adjust the coincidence count rate for the “yes”-answer (“ $x_1 = x_2$ ”). We perform about 200 projection measurements of equal states and calculate the average coincidence count rate between signal and idler photons. The simultaneous clicks in the idler and signal detectors means that the idler photon has been prepared in the state $|\psi(x_1)\rangle$ and has been successfully projected on the state $|\psi(x_2)\rangle$. We pick the average value as the threshold between “yes” and “no”. In this work, we experimentally evaluate collision probability for multiqudit quantum hash function with $q = 256$ and three groups of parameters: i) $d = 2$ and $m = 1, \dots, 7$, ii) $d = 3$ and $m = 1, \dots, 5$, and iii) $d = 4$ and $m = 1, \dots, 4$, i.e., we perform experiments with various number of qubits, qutrits and ququarts. We encode the classical message x_1 into the phase of states considered in Section 2.2. Since we are considering the worst-case situation, without loss of generality we can focus on the case when $x_2 = 0$. The value of x_1 corresponding to the worst-case scenario was calculated from

$$x_1 = \arg \max_{x \neq 0} \frac{1}{d^{2m}} \prod_{j=1}^m \left| 1 + e^{i\frac{2\pi s_{j,2}x}{q}} + \dots + e^{i\frac{2\pi s_{j,d}x}{q}} \right|^2 \quad (3.10)$$

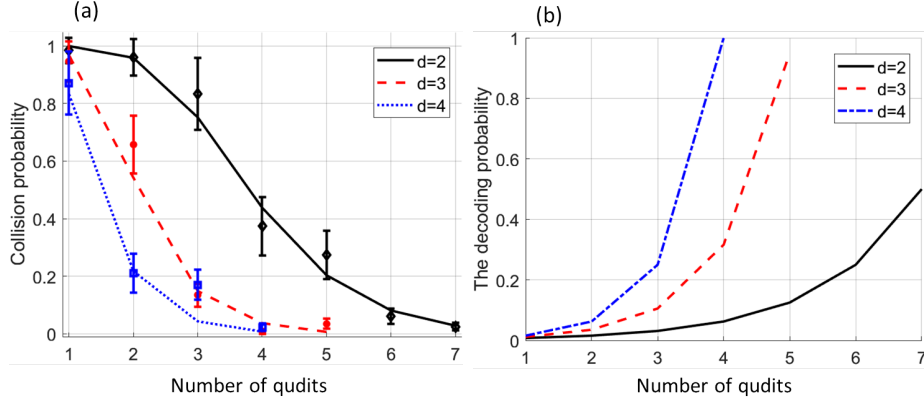


Figure 2. a) Comparing experimental and theoretical collision probabilities for the worst-case scenario for different dimensions of quantum states. b) The theoretical probability of extracting initial message from its quantum hash.

for an optimal (quasioptimal) set of parameters $\{s_{j,k}\}$, which in turn was precomputed as

$$\{s_{j,k}\} = \arg \min_{\{s_{j,k}\}} \max_{x \neq 0} \frac{1}{d^{2m}} \prod_{j=1}^m \left| 1 + e^{i \frac{2\pi s_{j,2} x}{q}} + \dots + e^{i \frac{2\pi s_{j,d} x}{q}} \right|^2. \quad (3.11)$$

Figure 2 shows the comparison of experimental and theoretical error rates for the worst-case scenario depending on different dimension of quantum states. The experimental results suggest that the proposed technique can be useful even for small sizes of input and output states. Moreover, it can be seen that the number of information carriers decreases with increase of their quantum state dimension for an optimal relation between collision probability and the decoding probability (the probability of extracting the classical input x from the quantum hash). For instance, if we limit the collision probability by 0.25 and the decoding probability by 0.15, the optimal number of qudits to “compress” a 8-bit classical information proves to be $m = 5$ for $d = 2$, $m = 3$ for $d = 3$, and $m = 2$ for $d = 4$. Moreover, according to the Holevo theorem [25] no more information can be extracted from a quantum d -level system than from a classical d -level system, which means that we have a bounded probability (below 1) to extract the information about classical input x .

4. Conclusion

In this paper, we have developed a high-dimensional quantum hashing protocol and presented its proof-of-principle implementation using orbital-angular momentum encoding of single photons. Experimental results agree quite well with the theoretical estimations of collision probability dependence on the number of qudits in a quantum hash. An important result is that the number of information carriers decreases with increase of their quantum state dimension for an optimal ratio between collision probability and the decoding probability.

Thus, the developed multiqudit quantum hashing approach can speed up quantum communications by reducing the number of particles being transferred while having balanced resistance to inversion and quantum collisions.

Acknowledgments

The experimental part of the work was made within the government assignment for FRC Kazan Scientific Center of RAS. The quantum hashing construction and analysis has been supported by the Kazan Federal University Strategic Academic Leadership Program (“PRIORITY-2030”). The authors express gratitude to Ehsan Shaghaei for valuable advice and programming support.

References

- [1] Christof Paar and Jan Pelzl. *Understanding Cryptography: A Textbook for Students and Practitioners*. Springer Publishing Company, Incorporated, 1st edition, 2009.
- [2] Jonathan Katz and Yehuda Lindell. *Introduction to Modern Cryptography, Second Edition*. CRC Press, 2014.
- [3] C.H. Bennett, G. Brassard, C. Crepeau, and U.M. Maurer. Generalized privacy amplification. *IEEE Transactions on Information Theory*, 41(6):1915–1923, 1995.
- [4] F.M. Ablayev and A.V. Vasiliev. Cryptographic quantum hashing. *Laser Physics Letters*, 11(2):025202, 2014.
- [5] Farid Ablayev, Marat Ablayev, Alexander Vasiliev, and Mansur Ziatdinov. Quantum fingerprinting and quantum hashing. computational and cryptographical aspects. *Baltic Journal of Modern Computing*, 4(4):860–875, 2016.
- [6] F Ablayev, M Ablayev, and A Vasiliev. On the balanced quantum hashing. *Journal of Physics: Conference Series*, 681(1):012019, 2016.
- [7] D. A. Turaykhanov, D. O. Akat’ev, A. V. Vasiliev, F. M. Ablayev, and A. A. Kalachev. Quantum hashing via single-photon states with orbital angular momentum. *Phys. Rev. A*, 104:052606, Nov 2021.
- [8] Alexander Vasiliev. Quantum hashing for finite abelian groups. *Lobachevskii Journal of Mathematics*, 37(6):751–754, 2016.
- [9] Joseph Naor and Moni Naor. Small-bias probability spaces: Efficient constructions and applications. In *Proceedings of the Twenty-second Annual ACM Symposium on Theory of Computing*, STOC ’90, pages 213–223, New York, NY, USA, 1990. ACM.
- [10] Noga Alon and Yuval Roichman. Random cayley graphs and expanders. *Random Structures & Algorithms*, 5(2):271–284, 1994.
- [11] Harry Buhrman, Richard Cleve, John Watrous, and Ronald de Wolf. Quantum fingerprinting. *Phys. Rev. Lett.*, 87(16):167902, Sep 2001.
- [12] Farid Ablayev and Marat Ablayev. On the concept of cryptographic quantum hashing. *Laser Physics Letters*, 12(12):125204, 2015.
- [13] Fulvio Flamini, Nicolò Spagnolo, and Fabio Sciarrino. Photonic quantum information processing: a review. *Reports on Progress in Physics*, 82(1):016001, nov 2018.
- [14] Alan E Willner, Kai Pang, Hao Song, Kaiheng Zou, and Huibin Zhou. Orbital angular momentum of light for communications. *Applied Physics Reviews*, 8(4):041312, 2021.
- [15] Manuel Erhard, Robert Fickler, Mario Krenn, and Anton Zeilinger. Twisted photons: new quantum perspectives in high dimensions. *Light: Science & Applications*, 7(3):17146–17146, 2018.

- [16] DN Klyshko. Utilization of vacuum fluctuations as an optical brightness standard. *Soviet Journal of Quantum Electronics*, 7(5):591, 1977.
- [17] CK Hong and Leonard Mandel. Experimental realization of a localized one-photon state. *Physical Review Letters*, 56(1):58, 1986.
- [18] Alois Mair, Alipasha Vaziri, Gregor Weihs, and Anton Zeilinger. Entanglement of the orbital angular momentum states of photons. *Nature Photonics*, 412:313–316, 2001.
- [19] Zeferino Ibarra-Borja, Carlos Sevilla-Gutiérrez, Roberto Ramírez-Alarcón, Qiwen Zhan, Hector Cruz-Ramírez, and Alfred B. U'Ren. Direct observation of oam correlations from spatially entangled bi-photon states. *Opt. Express*, 27(18):25228–25240, Sep 2019.
- [20] Eliot Bolduc, Nicolas Bent, Enrico Santamato, Ebrahim Karimi, and Robert W. Boyd. Exact solution to simultaneous intensity and phase encryption with a single phase-only hologram. *Opt. Lett.*, 38(18):3546–3549, Sep 2013.
- [21] E. V. Kovalkov, I. B. Bobrov, S. S. Straupe, and S. P. Kulik. Spatial bell-state generation without transverse mode subspace postselection. *Phys. Rev. Lett.*, 118:030503, Jan 2017.
- [22] Megan Agnew, Jonathan Leach, Melanie McLaren, F. Stef Roux, and Robert W. Boyd. Tomography of the quantum state of photons entangled in high dimensions. *Phys. Rev. A*, 84:062101, Dec 2011.
- [23] B Jack, J Leach, H Ritsch, S M Barnett, M J Padgett, and S Franke-Arnold. Precise quantum tomography of photon pairs with entangled orbital angular momentum. *New Journal of Physics*, 11(10):103024, oct 2009.
- [24] S. P. Walborn, A. N. de Oliveira, R. S. Thebaldi, and C. H. Monken. Entanglement and conservation of orbital angular momentum in spontaneous parametric down-conversion. *Phys. Rev. A*, 69:023811, Feb 2004.
- [25] Alexander S. Holevo. Some estimates of the information transmitted by quantum communication channel (russian). *Probl. Pered. Inform. [Probl. Inf. Transm.]*, 9(3):3–11, 1973.